How to cite: *Angew. Chem. Int. Ed.* **2023**, *62*, e202310357
doi.org/10.1002/anie.202310357

Self-Assembly

Controlling the Assembly of Cellulose-Based Oligosaccharides through Sequence Modifications

Nives Hribernik, Denisa Vargová, Marlene C. S. Dal Colle, Jia Hui Lim, Giulio Fittolani, Yang Yu, Junki Fujihara, Kai Ludwig, Peter H. Seeberger, Yu Ogawa, and Martina Delbianco**

Abstract: Peptides and nucleic acids with programmable sequences are widely explored for the production of tunable, self-assembling functional materials. Herein we demonstrate that the primary sequence of oligosaccharides can be designed to access materials with tunable shapes and properties. Synthetic cellulose-based oligomers were assembled into 2D or 3D rod-like crystallites. Sequence modifications within the oligosaccharide core influenced the molecular packing and led to the formation of square-like assemblies based on the rare cellulose IV_{II} allomorph. In contrast, modifications at the termini generated elongated aggregates with tunable surfaces, resulting in self-healing supramolecular hydrogels.

Nature generates complex systems via self-assembly of simpler components, encoding the assembly guidelines in the primary sequence of biomolecules.[1] Inspired by nature, chemists have designed synthetic analogues capable of self-assembling into beautiful architectures.[2] These systems are mostly based on peptide[3] and nucleic acid[4] oligomers, that can be easily synthesized with programmable sequences. By incorporating variations in the primary sequence, including non-canonical residues,[5] it is possible to precisely manipulate the morphology of supramolecular assemblies.[6] This versatility has enabled the creation of fibers,[7] particles,[8] sheets,[9] and more exotic architectures[10] with nanoscale control.

In contrast, synthetic carbohydrate supramolecular systems are mostly based on simple amphiphilic monomers[11] or polydisperse polysaccharides.[12] The assembly of oligosaccharides with uniform lengths and programmable sequences remained unexplored, primarily due to challenges associated with glycan synthesis.[13] Advances in automated synthetic methods[14] have facilitated the rapid generation of collections comprising both natural and non-natural oligosaccharides with controlled sequences. This newly accessible chemical space prompted us to explore the assembly of precision oligosaccharides. We postulated that certain sequences could assemble into well-defined nanomaterials and that specific modifications to such primary sequences could effectively govern the aggregation behavior of synthetic oligosaccharides, thus paving the way for programmable supramolecular oligosaccharide materials.

Cellulose, the most abundant organic material on earth that exists in several crystalline allomorphs, served as a starting point for our investigation.[15] We recently observed that a cellulose hexasaccharide ($\mathbf{A_6}$) self-assembled in aqueous solution into two-dimensional (2D) colloidal nanocrystals (Figure 1A).[16] The oligomers packed in a crystalline monolayer with the chain axis aligned perpendicularly to the lamellar plane in an anti-parallel fashion, permitting control over the crystal height, directly related to the length of the oligosaccharide chain. Upon drying, these platelets further aggregated into bundles with intrinsic chiral features. Still, the crystals were highly heterogeneous in the other dimensions and constituted only a small fraction of the entire sample.

To enhance the aggregation of cellulose oligomers and achieve a more homogeneous material, we employed an annealing step, a procedure commonly utilized to ensure the formation of regular structures in peptides and polymers.[17] Sonicated aqueous suspensions of $\mathbf{A_6}$ at different concentrations (Figure S5) were heated to 85 °C and kept at this temperature for 15 min, before being slowly cooled to 20 °C. Upon annealing, the 2 % (w/w) suspension generated long rod-like crystals, easily separable from the supernatant by centrifugation. About 80 % of the starting material was converted into crystals with length of ca. 1–2 μm and width of ca. 50–80 nm, while the supernatant contained residual

[*] N. Hribernik, D. Vargová, M. C. S. Dal Colle, G. Fittolani, Y. Yu, J. Fujihara, P. H. Seeberger, M. Delbianco
Department of Biomolecular Systems
Max Planck Institute of Colloids and Interfaces
Am Mühlenberg 1, 14476 Potsdam (Germany)
E-mail: martina.delbianco@mpikg.mpg.de
M. C. S. Dal Colle, J. Fujihara, K. Ludwig, P. H. Seeberger
Department of Chemistry and Biochemistry
Freie Universität Berlin
Arnimallee 22, 14195 Berlin (Germany)
J. H. Lim, Y. Ogawa
Univ. Grenoble Alpes
CNRS, CERMAV
38000 Grenoble (France)
E-mail: yu.ogawa@cermav.cnrs.fr

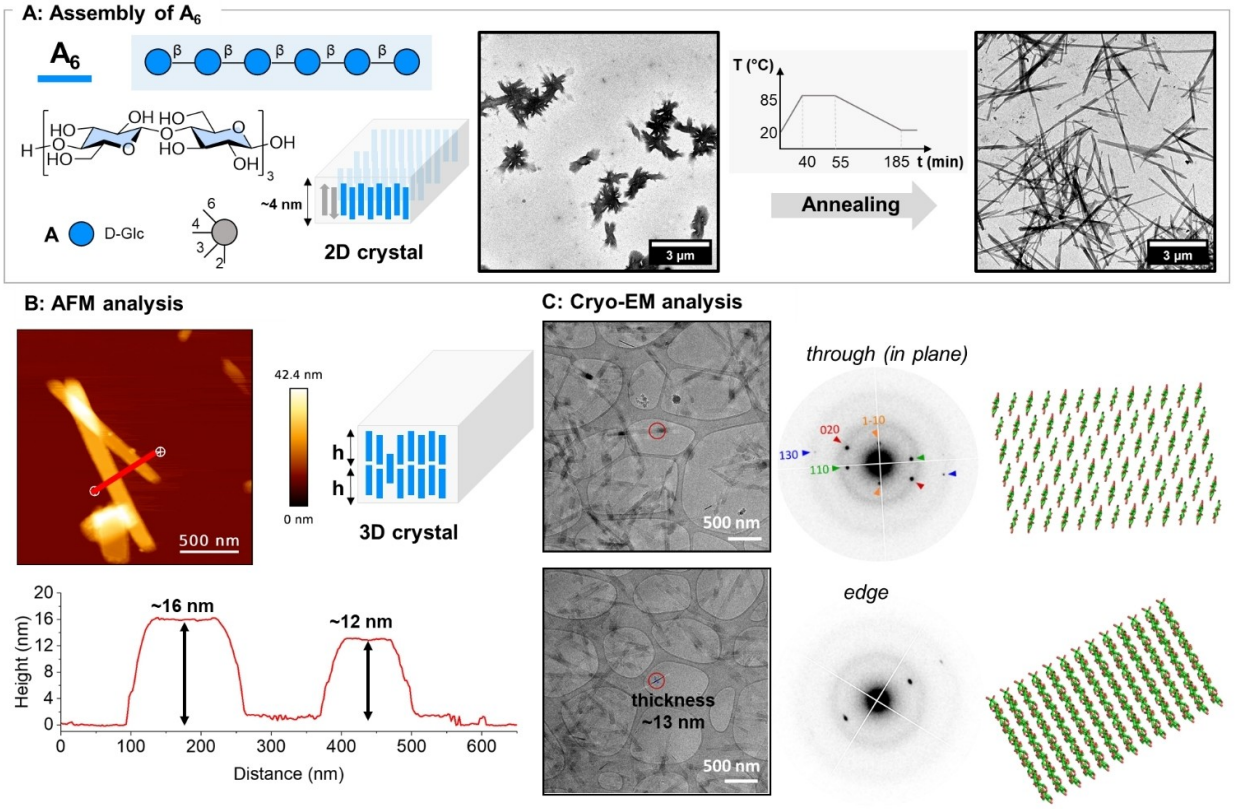

Figure 1. Assembly of cellulose hexamer $\mathbf{A_6}$. (A) $\mathbf{A_6}$ chemical structure and SNFG[19] representation, schematic representation of a 2D crystal, and TEM analysis of $\mathbf{A_6}$ assemblies before and after annealing. (B) AFM image and height (h) analysis indicated the formation of 3D crystals upon annealing of a 2% (w/w) aqueous suspension of $\mathbf{A_6}$. (C) Cryo-EM images and diffraction patterns obtained from the "through" and the "edge" views in the red circled area confirmed the presence of 3D crystallites with thickness of approximately 13 nm. The crystal structure models on the left column are in the crystallographic orientations corresponding to the respective diffraction patterns.

solubilized oligomers (Figure S6). Transmission electron microscopy (TEM) analysis confirmed the improved control over the lateral growth of the crystallites (Figure 1A). Atomic force microscopy (AFM) analysis indicated that the annealing process resulted in the growth of platelets in the height direction beyond the monolayer limit, leading to the formation of three-dimensional (3D) crystalline nanoparticles with heights ranging from 9 to 16 nm (Figure 1B and S8, the expected height of a 2D lamella of a cellulose hexamer is approximately 4 nm[16]). The 3D nature of the crystallites was further confirmed by cryo-TEM (Figure 1C). Diffraction patterns were obtained with an electron beam perpendicular (through) and parallel (edge) to the lamellar plane of different crystals in a vitrified ice layer. The "through" ED pattern demonstrated that the annealed crystals maintained the cellulose II crystal structure, as also indicated by XRD analysis[18] (Figure S4). The well-defined spot diffraction patterns in both views excluded the stacking of multiple crystalline domains along the thickness direction that would result in smeared diffraction pattern (Figure S10). This observation confirmed the single crystalline nature of the 3D crystals generated upon annealing. Further crystallographic analysis suggested that the 3D growth might be connected to individual chains shifting along the thickness direction, bridging multiple crystalline domains (Figure S9). This result demonstrates that either 2D or 3D nanomaterials can be produced from simple cellulose oligomers by simply changing the sample preparation protocol.

Equipped with a self-assembling model oligosaccharide and tools to control the assembly process, we explored whether systematic variations in the primary sequence could unlock novel morphologies. We hypothesized that introducing defects within the core of the cellulose oligomers could give rise to new allomorphs,[20] potentially yielding distinct crystallite shapes. In contrast, modifications at the oligomer termini should preserve the cellulose stacking core,[16] while impeding three-dimensional growth. The latter would also influence further supramolecular interactions between crystallites.

For the first approach, single modifications were installed within a cellulose octamer (Figure 2A), as we previously observed that more intense modifications resulted in amorphous structures.[21] Three cellulose-based oligomers (Figure S3) were synthesized by automated glycan assembly (AGA) from monosaccharide building blocks

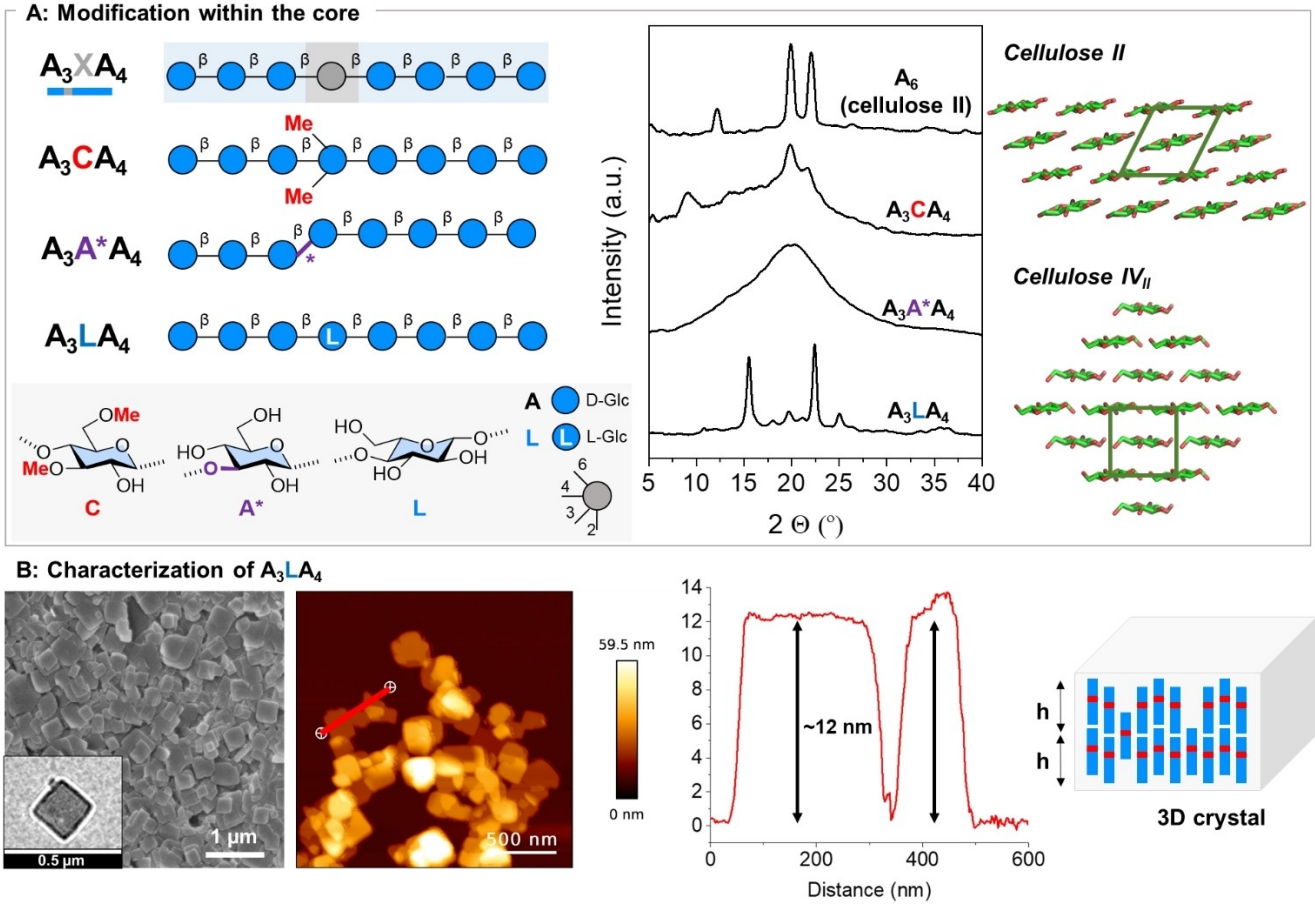

Figure 2. Synthetic cellulose oligomers with a single-site modification within the core. (A) SNFG representation, powder XRD analysis of compounds **A_3CA_4**, **$A_3A^*A_4$** and **A_3LA_4** and crystallographic differences between the cellulose II and cellulose IV_{II} allomorphs. (B) Characterization of **A_3LA_4** by SEM, TEM, and AFM with height measurement indicating the 3D nature of the crystallites.

(Figure S1 and S2). We analyzed the effect of non-canonical residues (**C**), variation in connectivity (**A***), and enantiomeric residues (**L**) by powder XRD analysis. While some modifications resulted in amorphous (**$A_3A^*A_4$**) or low crystalline (**A_3CA_4**) materials, the introduction of a single L-glucose unit led to a cellulose IV_{II} type structure.[22] In cellulose IV_{II}, the oligomers maintain the antiparallel orientation yet with larger intermolecular spacing, with a consequent formation of an orthorhombic unit cell (Figure 2A).[23] SEM, TEM, and AFM imaging showed that the 2 % (w/w) annealed suspension of **A_3LA_4** assembled into nano-squares (Figure 2B), that measured ca. 50–200 nm in lateral directions. AFM height analysis suggested the 3D nature of the crystallites (Figure S13) with heights between 8 and 16 nm. The ED pattern of **A_3LA_4** single crystal showed well-resolved diffraction with a higher resolution (at near 1 Å) than the previous ED patterns obtained from natural cellulose IV_{II} crystals (Figure S16).[23] The insertion of L-glucose residue thus improved the crystalline ordering of molecules. The refinement of the crystal structure is currently underway to reveal the molecular details of cellulose IV_{II} packing. This finding highlights single-site modification as a valuable approach for guiding the aggregation of oligosaccharides and facilitating the design of novel morphologies.

The second series of oligosaccharides (Figure 3A) was designed based on the hypothesis that by introducing non-canonical residues at the oligomer termini, three-dimensional crystal growth can be hindered effectively, while preserving the interaction between the cellulose cores.[24] We synthesized a series of oligosaccharides featuring an eight-glucose unit core, wherein the reducing and non-reducing ends were modified with different monomers (either a 3,6-methylated glucose **C** or a mannose unit **M**, Figure 3A and S3).

Powder XRD analysis confirmed the cellulose II type structures for all three compounds (Figure 3A), proving that the external modifications did not notably alter the packing of the molecules within the crystal. Annealing triggered the formation of elongated platelets (ca. 500 nm long, Figure 3B) that appeared thinner and more flexible in comparison to the long, rigid crystallites obtained from **A_6**. AFM analysis indicated that the height of the crystals obtained from all three compounds corresponded to the length of the single oligosaccharide chain (Figure 3B and S18). This was additionally confirmed by measuring the thickness of a

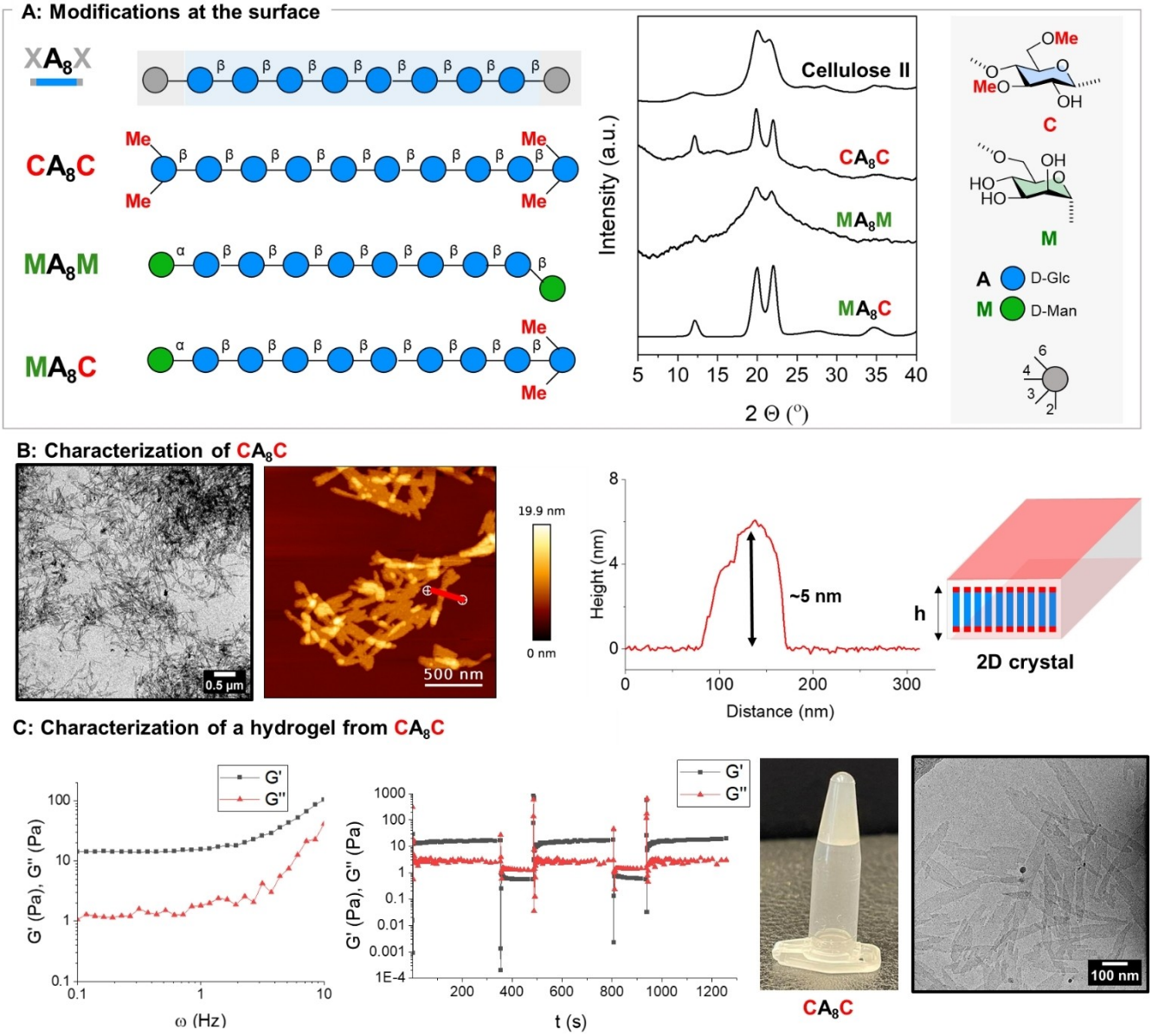

Figure 3. Synthetic oligomers with a cellulose core and modifications at the termini. (A) SNFG representation and powder XRD analysis of compounds **CA_8C**, **MA_8M** and **MA_8C**. (B) Characterization of compound **CA_8C** by TEM, and AFM height analysis indicating the 2D nature of the crystallites. (C) Rheometric characterization of the 2% (w/w) hydrogel of **CA_8C** by frequency sweep, sequential step strain sweeps at 25 °C showing self-healing behaviour of the hydrogel, photo of the 2% (w/w) hydrogel, and cryo-TEM image of the 0.5% (w/w) hydrogel.

single crystal of **CA_8C** in cryo-electron tomography (Figure S20 and Movie S1). Thus, the modifications at the termini effectively hindered three-dimensional crystal growth, promoting the formation of 2D assemblies.

Upon annealing, the 2% (w/w) suspensions of compounds **CA_8C** and **MA_8C** transformed into opaque hydrogels, as confirmed by rheometric measurements (Figure 3C). The 2% (w/w) samples of both compounds displayed a typical gel behavior in a frequency sweep experiment, with the storage modulus G′ of approx. 10 Pa (Figure S21). Crystal length and hydrogel stiffness could be tuned with the oligomer concentration, with shorter platelets (around 100 nm) and weaker gels (G' around 1 Pa) obtained upon annealing of a 0.5% (w/w) suspension (Figure S22). Both **CA_8C** and **MA_8C** gels showed self-healing behavior after being exposed to high shear strain in a step strain experiment (Figure 3C and S21). The platelets formed by compound **MA_8M** precipitated out of solution, suggesting that 3,6-methylated glucose unit **C** on the surface of the platelets was required for hydrogel formation. This result proves that oligosaccharide sequences can be designed to assemble into functional materials with tunable surfaces.

Overall, we demonstrate the programmability of oligosaccharide self-assembly through strategic modifications in the primary sequence of synthetic cellulose derivatives. By combining specific structural alterations and careful sample

preparation procedures, we achieved precise control over the morphology of the fabricated material, resulting in tunable 2D and 3D nanostructures. Internal modifications altered the natural packing of cellulose oligosaccharides and led to the formation of square-shaped nanostructures, based on the rare cellulose IV_{II} allomorph. This approach holds promise for exploring other poorly characterized, or not yet discovered, polysaccharide allomorphs. Additionally, we designed sequences that preserved the natural packing of cellulose oligomers to generate nanocrystals with non-cellulosic surfaces. The exploration of other oligosaccharide sequences and assembly procedures will put oligosaccharides on the map of sequence-programmable oligomers,[25] side by side to peptides and nucleic acids, offering new tools to material scientists and supramolecular chemists.

Supporting Information

The authors have cited additional references within the Supporting Information.[26–34]

Acknowledgements

We thank the Max Planck Society, the German Federal Ministry of Education and Research (BMBF, grant number 13XP5114), the Deutsche Forschungsgemeinschaft (DFG, German Research Foundation—SFB 1449-431232613; subproject C2 and TP701), and the European Research Council (ERC) under the Horizon Europe research and innovation programme (Project 101075357—GLYCOFOLD) for generous financial support. JHL and YO acknowledge Agence Nationale de la Recherche (ANR grant number: ANR-21-CE29-0016-1) and Glyco@Alps (ANR-15-IDEX-02) for the financial support and the NanoBio-ICMG platform (FR 2607) for granting access to the electron microscopy facility. Open Access funding enabled and organized by Projekt DEAL.

Conflict of Interest

The authors declare no conflict of interest.

Data Availability Statement

All data supporting the findings of this study are available within the article and in the Supporting Information files. Raw data for NMR analysis, XRD and rheometric measurements can be downloaded from https://doi.org/10.17617/3.RRVHKQ, Edmond.

Keywords: Biomaterials · Cellulose · Hydrogels · Oligosaccharides · Self-Assembly

[1] a) G. M. Whitesides, J. P. Mathias, C. T. Seto, *Science* **1991**, *254*, 1312–1319; b) P. Fratzl, R. Weinkamer, *Prog. Mater. Sci.* **2007**, *52*, 1263–1334; c) A. C. Mendes, E. T. Baran, R. L. Reis, H. S. Azevedo, *WIREs Nanomed. Nanobiotechnol.* **2013**, *5*, 582–612.

[2] a) J. D. Hartgerink, E. Beniash, S. I. Stupp, *Science* **2001**, *294*, 1684–1688; b) S. C. Glotzer, M. J. Solomon, *Nat. Mater.* **2007**, *6*, 557–562; c) A. Travesset, *Science* **2011**, *334*, 183–184; d) T. Aida, E. W. Meijer, S. I. Stupp, *Science* **2012**, *335*, 813–817; e) L. Cademartiri, K. J. M. Bishop, *Nat. Mater.* **2015**, *14*, 2–9; f) P. W. J. M. Frederix, G. G. Scott, Y. M. Abul-Haija, D. Kalafatovic, C. G. Pappas, N. Javid, N. T. Hunt, R. V. Ulijn, T. Tuttle, *Nat. Chem.* **2015**, *7*, 30–37; g) E. Gazit, *Nat. Chem.* **2015**, *7*, 14–15; h) F. Praetorius, H. Dietz, *Science* **2017**, *355*, eaam5488.

[3] a) H.-S. Jang, J.-H. Lee, Y.-S. Park, Y.-O. Kim, J. Park, T.-Y. Yang, K. Jin, J. Lee, S. Park, J. M. You, K.-W. Jeong, A. Shin, I.-S. Oh, M.-K. Kwon, Y.-I. Kim, H.-H. Cho, H. N. Han, Y. Kim, Y. H. Chang, S. R. Paik, K. T. Nam, Y.-S. Lee, *Nat. Commun.* **2014**, *5*, 3665; b) T. Jiang, C. Xu, Y. Liu, Z. Liu, J. S. Wall, X. Zuo, T. Lian, K. Salaita, C. Ni, D. Pochan, V. P. Conticello, *J. Am. Chem. Soc.* **2014**, *136*, 4300–4308; c) E. L. Magnotti, S. A. Hughes, R. S. Dillard, S. Wang, L. Hough, A. Karumbamkandathil, T. Lian, J. S. Wall, X. Zuo, E. R. Wright, V. P. Conticello, *J. Am. Chem. Soc.* **2016**, *138*, 16274–16282; d) Y. Lin, M. R. Thomas, A. Gelmi, V. Leonardo, E. T. Pashuck, S. A. Maynard, Y. Wang, M. M. Stevens, *J. Am. Chem. Soc.* **2017**, *139*, 13592–13595; e) A. M. Garcia, M. Melchionna, O. Bellotto, S. Kralj, S. Semeraro, E. Parisi, D. Iglesias, P. D'Andrea, R. De Zorzi, A. V. Vargiu, S. Marchesan, *ACS Nano* **2021**, *15*, 3015–3025.

[4] a) P. W. K. Rothemund, *Nature* **2006**, *440*, 297–302; b) P. Wang, S. Gaitanaros, S. Lee, M. Bathe, W. M. Shih, Y. Ke, *J. Am. Chem. Soc.* **2016**, *138*, 7733–7740; c) L. L. Ong, N. Hanikel, O. K. Yaghi, C. Grun, M. T. Strauss, P. Bron, J. Lai-Kee-Him, F. Schueder, B. Wang, P. Wang, J. Y. Kishi, C. Myhrvold, A. Zhu, R. Jungmann, G. Bellot, Y. Ke, P. Yin, *Nature* **2017**, *552*, 72–77; d) H. Yu, D. T. L. Alexander, U. Aschauer, R. Häner, *Angew. Chem. Int. Ed.* **2017**, *56*, 5040–5044.

[5] a) T. A. Martinek, F. Fülöp, *Chem. Soc. Rev.* **2012**, *41*, 687–702; b) M. Szefczyk, *Nanoscale* **2021**, *13*, 11325–11333.

[6] A. Lampel, R. V. Ulijn, T. Tuttle, *Chem. Soc. Rev.* **2018**, *47*, 3737–3758.

[7] a) E. T. Pashuck, H. Cui, S. I. Stupp, *J. Am. Chem. Soc.* **2010**, *132*, 6041–6046; b) B. N. S. Thota, X. Lou, D. Bochicchio, T. F. E. Paffen, R. P. M. Lafleur, J. L. J. van Dongen, S. Ehrmann, R. Haag, G. M. Pavan, A. R. A. Palmans, E. W. Meijer, *Angew. Chem. Int. Ed.* **2018**, *57*, 6843–6847.

[8] R. J. Macfarlane, B. Lee, M. R. Jones, N. Harris, G. C. Schatz, C. A. Mirkin, *Science* **2011**, *334*, 204–208.

[9] a) T. Jiang, C. Xu, X. Zuo, V. P. Conticello, *Angew. Chem. Int. Ed.* **2014**, *53*, 8367–8371; b) J. Lee, I. R. Choe, N.-K. Kim, W.-J. Kim, H.-S. Jang, Y.-S. Lee, K. T. Nam, *ACS Nano* **2016**, *10*, 8263–8270.

[10] a) B. Liu, C. G. Pappas, E. Zangrando, N. Demitri, P. J. Chmielewski, S. Otto, *J. Am. Chem. Soc.* **2019**, *141*, 1685–1689; b) C. G. Pappas, B. Liu, I. Marić, J. Ottelé, A. Kiani, M. L. van der Klok, P. R. Onck, S. Otto, *J. Am. Chem. Soc.* **2021**, *143*, 7388–7393.

[11] a) A. Chen, I. S. Okafor, C. Garcia, G. Wang, *Carbohydr. Res.* **2018**, *461*, 60–75; b) A. Brito, S. Kassem, R. L. Reis, R. V. Ulijn, R. A. Pires, I. Pashkuleva, *Chem* **2021**, *7*, 2943–2964; c) H. Li, M. Mumtaz, T. Isono, T. Satoh, W.-C. Chen, R. Borsali, *Polym. J.* **2022**, *54*, 455–464.

[12] a) S. Hornig, T. Heinze, *Biomacromolecules* **2008**, *9*, 1487–1492; b) S. Hornig, T. Heinze, C. R. Becer, U. S. Schubert, *J. Mater. Chem.* **2009**, *19*, 3838–3840; c) S. C. Fox, B. Li, D. Xu, K. J. Edgar, *Biomacromolecules* **2011**, *12*, 1956–1972; d) K. Petzold-Welcke, K. Schwikal, S. Daus, T. Heinze, *Carbohydr. Polym.* **2014**, *100*, 80–88; e) P. Schulze, M. Gericke, F. Scholz, H. Wondraczek, P. Miethe, T. Heinze, *Macromol. Chem. Phys.* **2016**, *217*, 1823–1833.
[13] a) T. J. Boltje, T. Buskas, G.-J. Boons, *Nat. Chem.* **2009**, *1*, 611–622; b) P. H. Seeberger, *Nat. Chem. Biol.* **2009**, *5*, 368–372.
[14] a) M. Panza, S. G. Pistorio, K. J. Stine, A. V. Demchenko, *Chem. Rev.* **2018**, *118*, 8105–8150; b) M. Guberman, P. H. Seeberger, *J. Am. Chem. Soc.* **2019**, *141*, 5581–5592; c) J.-Y. Huang, M. Delbianco, *Synthesis* **2022**, *55*, 1337–1354; d) W. Yao, D.-C. Xiong, Y. Yang, C. Geng, Z. Cong, F. Li, B.-H. Li, X. Qin, L.-N. Wang, W.-Y. Xue, N. Yu, H. Zhang, X. Wu, M. Liu, X.-S. Ye, *Nat. Synth.* **2022**, *1*, 854–863.
[15] P. Zugenmaier, *Cellulose*, 1 ed, Springer, Berlin, Heidelberg **2008**, pp. 101–171.
[16] G. Fittolani, D. Vargová, P. H. Seeberger, Y. Ogawa, M. Delbianco, *J. Am. Chem. Soc.* **2022**, *144*, 12469–12475.
[17] a) X. Wang, G. Guerin, H. Wang, Y. Wang, I. Manners, M. A. Winnik, *Science* **2007**, *317*, 644–647; b) J. M. Godbe, R. Freeman, L. F. Burbulla, J. Lewis, D. Krainc, S. I. Stupp, *ACS Biomater. Sci. Eng.* **2020**, *6*, 1196–1207; c) M. Wada, S. Wakiya, K. Kobayashi, S. Kimura, M. Kitaoka, R. Kusumi, F. Kimura, T. Kimura, *Cellulose* **2021**, *28*, 6757–6765.
[18] a) P. Langan, Y. Nishiyama, H. Chanzy, *J. Am. Chem. Soc.* **1999**, *121*, 9940–9946; b) P. Langan, N. Sukumar, Y. Nishiyama, H. Chanzy, *Cellulose* **2005**, *12*, 551–562; c) P. Chen, Y. Ogawa, Y. Nishiyama, M. Bergenstråhle-Wohlert, K. Mazeau, *Cellulose* **2015**, *22*, 1485–1493.
[19] A. Varki, R. D. Cummings, M. Aebi, N. H. Packer, P. H. Seeberger, J. D. Esko, P. Stanley, G. Hart, A. Darvill, T. Kinoshita, J. J. Prestegard, R. L. Schnaar, H. H. Freeze, J. D. Marth, C. R. Bertozzi, M. E. Etzler, M. Frank, J. F. Vliegenthart, T. Lütteke, S. Perez, E. Bolton, P. Rudd, J. Paulson, M. Kanehisa, P. Toukach, K. F. Aoki-Kinoshita, A. Dell, H. Narimatsu, W. York, N. Taniguchi, S. Kornfeld, *Glycobiology* **2015**, *25*, 1323–1324.
[20] P. de Andrade, J. C. Muñoz-García, G. Pergolizzi, V. Gabrielli, S. A. Nepogodiev, D. Iuga, L. Fábián, R. Nigmatullin, M. A. Johns, R. Harniman, S. J. Eichhorn, J. Angulo, Y. Z. Khimyak, R. A. Field, *Chem. Eur. J.* **2021**, *27*, 1374–1382.
[21] Y. Yu, T. Tyrikos-Ergas, Y. Zhu, G. Fittolani, V. Bordoni, A. Singhal, R. J. Fair, A. Grafmüller, P. H. Seeberger, M. Delbianco, *Angew. Chem. Int. Ed.* **2019**, *58*, 13127–13132.
[22] a) A. D. French, S. Pérez, V. Bulone, T. Rosenau, D. Gray, in *Encyclopedia of Polymer Science and Technology*, Wiley, Hoboken **2002**, pp. 1–69; b) P. Zugenmaier, *Prog. Polym. Sci.* **2001**, *26*, 1341–1417.
[23] A. Buleon, H. Chanzy, *J. Polym. Sci. Polym. Phys. Ed.* **1980**, *18*, 1209–1217.
[24] A. D. Merg, G. Touponse, E. van Genderen, X. Zuo, A. Bazrafshan, T. Blum, S. Hughes, K. Salaita, J. P. Abrahams, V. P. Conticello, *Angew. Chem. Int. Ed.* **2019**, *58*, 13507–13512.
[25] B. van Genabeek, B. A. G. Lamers, C. J. Hawker, E. W. Meijer, W. R. Gutekunst, B. V. K. J. Schmidt, *J. Polym. Sci.* **2021**, *59*, 373–403.
[26] S. Eller, M. Collot, J. Yin, H. S. Hahm, P. H. Seeberger, *Angew. Chem. Int. Ed.* **2013**, *52*, 5858–5861.
[27] P. Dallabernardina, F. Schuhmacher, P. H. Seeberger, F. Pfrengle, *Org. Biomol. Chem.* **2016**, *14*, 309–313.
[28] Y. Yu, S. Gim, D. Kim, Z. A. Arnon, E. Gazit, P. H. Seeberger, M. Delbianco, *J. Am. Chem. Soc.* **2019**, *141*, 4833–4838.
[29] K. Le Mai Hoang, A. Pardo-Vargas, Y. Zhu, Y. Yu, M. Loria, M. Delbianco, P. H. Seeberger, *J. Am. Chem. Soc.* **2019**, *141*, 9079–9086.
[30] M. Gude, J. Ryf, P. D. White, *Lett. Pept. Sci.* **2002**, *9*, 203–206.
[31] M. Guberman, M. Bräutigam, P. H. Seeberger, *Chem. Sci.* **2019**, *10*, 5634–5640.
[32] M. Hurevich, J. Kandasamy, B. M. Ponnappa, M. Collot, D. Kopetzki, D. T. McQuade, P. H. Seeberger, *Org. Lett.* **2014**, *16*, 1794–1797.
[33] D. N. Mastronarde, *Microsc. Microanal.* **2003**, *9*, 1182–1183.
[34] J. Schindelin, I. Arganda-Carreras, E. Frise, V. Kaynig, M. Longair, T. Pietzsch, S. Preibisch, C. Rueden, S. Saalfeld, B. Schmid, J.-Y. Tinevez, D. J. White, V. Hartenstein, K. Eliceiri, P. Tomancak, A. Cardona, *Nat. Methods* **2012**, *9*, 676–682.

Manuscript received: July 20, 2023
Accepted manuscript online: October 12, 2023
Version of record online: October 25, 2023